

Active Rendezvous for Multi-Robot Pose Graph Optimization using Sensing over Wi-Fi

Weiying Wang¹, Ninad Jadhav¹, Paul Vohs¹, Nathan Hughes², Mark Mazumder², and Stephanie Gil¹

¹ Arizona State University, Tempe AZ 85004, USA,

² MIT Lincoln Laboratory, Lexington, MA 02421, USA

Abstract. We present a novel framework for collaboration amongst a team of robots performing Pose Graph Optimization (PGO) that addresses two important challenges for multi-robot SLAM: that of enabling information exchange “on-demand” via *active rendezvous*, and that of rejecting outlier measurements with high probability. Our key insight is to exploit relative position data present in the communication channel between agents, as an independent measurement in PGO. We show that our algorithmic and experimental framework for integrating Channel State Information (CSI) over the communication channels, with multi-agent PGO, addresses the two open challenges of enabling information exchange and rejecting outliers. Our presented framework is distributed and applicable in low-lighting or featureless environments where traditional sensors often fail. We present extensive experimental results on actual robots showing both the use of *active rendezvous* resulting in error reduction by 6X as compared to randomly occurring rendezvous and the use of CSI observations providing a reduction in ground truth pose estimation errors of 32%. These results demonstrate the promise of using a combination of multi-robot coordination and CSI to address challenges in multi-agent localization and mapping – providing an important step towards integrating communication as a novel sensor for SLAM tasks.

Keywords: Rendezvous, Multi-robot SLAM, Sensing, Wi-Fi, Robotics

1 Introduction

Multi-robot mapping allows quick exploration of unknown environments and resiliency to failures. As a result there has been a significant effort to establish the necessary coordination algorithms for efficient and accurate mapping using information fused from teams of robots [21, 6, 22, 20]. A common and critical assumption in these works is that agents can share information in a reliable manner and that relative position information is sufficiently accurate to allow for integration of data [6, 21]. In practice however,

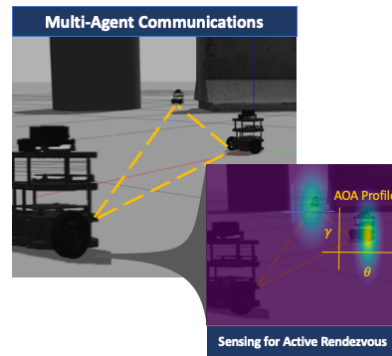


Fig. 1: *Sensor information from wireless signals used for multi-robot PGO.*

ensuring these assumptions is very challenging. For information exchange, random rendezvous opportunities are often exploited, or it is assumed that agents can navigate to a common location in the map [20, 11, 21]. However, the question of how to enforce a communication rendezvous in a *distributed* fashion that does not require agents to have a known map, i.e. that is *independent of the environment*, remains an open question. When validating shared observations, outliers in estimated relative pose measurements between agents can easily result from data mismatch and aliasing errors. The problem of detecting outliers has been recently identified as one of the open problems for the next era of multi-robot simultaneous localization and mapping, penned the “robust-perception age” [1]. The authors in [1] describe the tenuous nature of this problem where even a single outlier can dramatically degrade the quality of the pose estimates. This degradation of quality leads to the inability to detect outliers in future measurements, as well as instability and eventual divergence of the estimation process [3].

Ideally, it would be possible to address these challenges by using partial, local information – an objective that was recently identified as an important open problem for robust distributed mapping [1]. By building upon a key insight, that the communication link between agents contains valuable relative position information that can be fruitfully exploited in PGO, we address these challenges problems from a new perspective. Specifically, we build upon our prior work that uses Channel State Information (CSI) observations collected over communication links between agents to derive *angle-of-arrival* (AOA) information for received communication signals without the need for specialized hardware [7, 14]. This paper develops a novel framework for integrating this information with pose-graph optimization to address two important problems of 1) realizing data exchange on demand, or *active rendezvous*, between agents in a way that maintains pose estimation errors below a desired threshold, and 2) mitigating the effect of outlier measurements on PGO and improving the global (ground truth) accuracy of PGO methods. Importantly, our methods are distributed and applicable to featureless and low-light environments where vision-based methods may fail.

We develop an algorithmic framework for enforcing *active rendezvous* and for mitigating outliers in relative pose estimates between agents during a pose-graph optimization task. Our active rendezvous algorithm monitors internal error estimates for each agent as they move through the environment. Whenever an agent’s internal error passes a user specified threshold, the agent engages in an adaptive networking trajectory [7] where it uses local angle-of-arrival (AOA) information to navigate towards directions that improve its actual data rate to a selected communication neighbor. As such, our algorithm does not require agents to agree on a meeting location and operates in a distributed manner. For outlier mitigation, we selectively weight the information matrix of a relative pose measurement using the likelihood that a relative pose estimate is accurate as compared to the AOA information (an independent measurement over the wireless signal). We show that the incorporation of AOA information results in an improvement of estimation accuracy of 32% with respect to ground truth of hardware experiments. Finally, this paper begins to lay the foundation for using

communication-as-a-sensor for multi robot PGO and coordinated mapping tasks.

Paper Contributions: 1) an algorithm for achieving *active rendezvous* that is independent of the environment 2) a framework for using AOA information to mitigate the effect of outlier measurements on during a pose graph optimization task 3) a thorough experimental validation of all claims.

2 Related Work

As noted in [1], Pose Graph Optimization (PGO) is one of the most common modern techniques for SLAM, and supports many crucial tasks in robotics. A variety of techniques exist to extend PGO methods to multi-robot mapping problems. Choudhary et al address the limited communication challenge in [4] by exchanging semantic information between agents to avoid exchanging raw sensor data. In [18], convex optimization for graph sparsification is used to address the challenges of acoustic communication channels. Techniques for reducing the amount of poses considered are leveraged in [5, 13, 16] to reduce bandwidth requirements. However, these techniques still suffer from outlier observations and the inability to coordinate higher rates of information exchange on demand.

Additionally, there is a large body of work focused on light-weight position estimation from Radio Frequency (RF) signals. For instance, RF localization has been successfully applied to positioning when access to GPS signals are unavailable, such as indoor environments [12, 17], but requires the presence of known anchors. Decentralized localization without the use of beacons or anchor points can be achieved through range [28] and vectorial distance estimation [24] via time-of-arrival and time-difference-of-arrival techniques for multilateration. Angle-of-arrival measurements can also be used for estimating orientation [19]. Synthetic aperture radar (SAR) techniques have been used for indoor positioning in the presence of multipath and alleviate the need for bulky multi-antenna arrays [14, 15, 7, 27], which shows great promise for robotic applications.

As a supplement to some of the challenges of passive estimation, active SLAM approaches attempt to incorporate estimation uncertainty into the control of agents. This can include monitoring the estimation divergence during exploration [3] and estimating information-gain from exploration versus uncertainty reduction via repeated visitations [26, 25] using pose graphs. However, almost all active SLAM approaches rely on an explicit model of the environment.

In contrast to other outlined mapping and localization approaches, this paper highlights an algorithmic and experimental framework to intelligently incorporate collaborative mapping techniques into PGO for collaborative mapping. Our approach is independent of the environment or known anchors and allows for coordination to improve estimation quality in the presence of uncertainty.

3 Problem Statement

We wish to design an approach for collaborative mapping of an environment where n robots explore an unknown environment and must maintain accurate estimates of their pose. Here robot i 's pose is given by $x_i(t) := (R_i(t), p_i(t))$

where $p_i(t) \in \mathbb{R}^3$ is the position of agent i at time t and $R_i(t) \in SO(3)$ is the orientation of agent i at time t . $SO(3)$ here is the special orthogonal group, defined as $\{R \in \mathbb{R}^{3 \times 3} : R^\top R = I_3, \det(R) = 1\}$. In order to prevent divergence of the estimation process, these robots must periodically exchange information with one another through rendezvous to improve their estimated trajectories. We assume that rendezvous between two agents i and j can occur whenever there exists a communication link between robots that can support the required data rate $q_i \geq 0$ in Mb/s for exchanging enough information to reduce the estimation error of the agent. In practice this value is dependent on the nature of the data to be exchanged. We make a distinction between the communication rate required for rendezvous, versus the minimum communication rate required to “sense”, or send a ping, to another agent. Importantly, the latter is often possible at much larger distances than the former. We define the set of robots with which agent i has minimal connectivity to as $\mathcal{N}_{C_i}(t)$; agents in this neighborhood can transmit pings to one another (a minimum rate of about 6Mb/s) but may not be able to transmit other data. Finally, we define a *service discrepancy* as:

$$w_{ij} = \max\left(\frac{\alpha_i(q_i - \rho_{ij})}{q_i}, 0\right) \quad (1)$$

where $\alpha_i \geq 0$ is the importance weight of agent i , and $\rho_{ij} \geq 0$ is the actual capacity of the link between i and j in Mb/s. A service discrepancy $w_{ij} = 0$ denotes that agent j can transmit data to agent i at its desired data rate q_i .

3.1 Pose Graph Optimization

We assume that each robot acquires relative pose measurements which will be denoted $\bar{z}_j^i(t)$ where the sub and super-scripts denote the relative observation of j with respect to the reference frame of robot i at time t . We follow the observation model from [4], dropping t for clarity:

$$\bar{z}_j^i := (\bar{R}_j^i, \bar{p}_j^i), \text{ where } \bar{R}_j^i = (R_i)^\top R_j R_\epsilon \text{ and } \bar{p}_j^i = (R_i)^\top (p_j - p_i) + p_\epsilon \quad (2)$$

Here (R_ϵ, p_ϵ) denotes the noise of the observation and, roughly speaking, is assumed to be drawn from some zero-mean Gaussian distribution with Fisher information matrix $\Omega_{\bar{z}_j^i(t)}$. It is important to note the (R_j, p_j) are not necessarily from the same time t as $\bar{z}_j^i(t)$ is. This allows for odometry of a single robot or relative pose estimates from observed landmarks to be captured with the same notation. We define $\mathcal{E}_{\bar{z}}(t)$ as the set of all relative pose observations for all agents up to time t , and $\mathcal{E}_{\bar{z}(t)}^i$ as the subset of $\mathcal{E}_{\bar{z}}(t)$ relative to agent i . We also define $\mathcal{X}_i(t)$ as the set of all poses of robot i up to time t .

We assume the agents are capable of an estimation process to find an optimized set of poses x^* following the maximum likelihood formulation:

$$x^* = \arg \max_x \prod_{\bar{z} \in \mathcal{E}_{\bar{z}}} L(\bar{z}|x) \quad (3)$$

Our development is largely independent of the actual method to obtain x^* and thus we keep the concepts general where possible. We refer the interested reader to [4, 9] for example methods for obtaining x^* . We assume that the method to obtain x^* allows for any individual robot i to obtain an error metric for

the estimation process at any time, denoted as $Err_i(t, \mathcal{X}_i(t), \mathcal{E}_{\bar{z}}^i(t))$. One such example that follows from (3) is:

$$Err_i(t, \mathcal{X}_i(t), \mathcal{E}_{\bar{z}}^i(t)) := \sum_{\bar{z} \in \mathcal{E}_{\bar{z}}^i(t)} \omega_p^2 \|p_j - p_i - R_i \bar{p}_j\|^2 + \frac{\omega_R^2}{2} \|R_j - R_i \bar{R}_j\|_F^2 \quad (4)$$

where $\|\cdot\|_F^2$ is the Frobenius norm and ω_p^2 and $\frac{\omega_R^2}{2}$ are concentration parameters for the distribution of R_ϵ, p_ϵ , as discussed in [4].

In addition to traditional observations for pose optimization, we derive a framework for incorporating a new observation type: observations over wireless channels between communicating robots. In particular, we leverage previous work on attaining directional signal profiles, or *angle-of-arrival* information for each communicating pair of agents [7]. A primer on how to attain the angle-of-arrival profile F_{ij} for each pair of communicating agents is included in Sec. 4.

Our goal is to ensure that once the estimation error passes a user defined threshold $\delta > 0$, a subset of the agents can engage in active rendezvous to exchange information to reduce overall estimation errors. We stress that the concepts of this paper are extensible beyond Equation (4) to any error metric Err_i that can be computed directly from the estimation process.

Problems Addressed: In this paper our objectives are two-fold: for every robot $i \in \{1, \dots, n\}$ with the local information of observations $\mathcal{E}_{\bar{z}}^i$ and observations over the wireless channel of F_{ij} for all j in \mathcal{N}_{C_i} we aim to:

Problem 1 (Active Rendezvous). Develop an algorithm for achieving active rendezvous between agents that is independent of the acquired map.

Problem 2 (Outlier Rejection). Develop a framework that uses observations over the wireless channels, F_{ij} , to mitigate outlier observations in $\bar{z}_j^i(t)$.

4 Primer: Angle-of-Arrival in Multi-Robot Systems

As agents communicate, messages are transmitted over wireless channels h which are complex numbers exposed by some commodity Wi-Fi cards and measurable from any wireless device. These quantities characterize the power and phase of a received signal, and are affected by the path the signal traverses (attenuation) and the environment (scattering, multi-path), which can reveal information about the direction of the signal's source. Attaining angle-of-arrival (AOA) information requires using an array of multiple antennas that are normally too bulky for small, agile robot platforms. Fortunately, previous work demonstrates that the combination of robot motion and wireless channel measurements

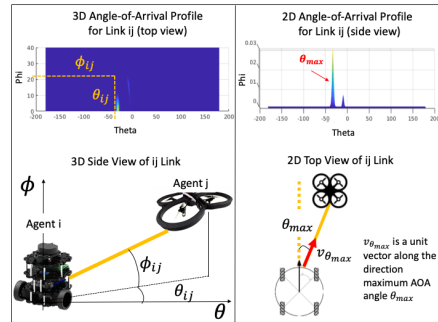


Fig. 2: AOA information in signal profile using Channel State Information (CSI).

can obtain the functionality of a multi-antenna array on a small robot platform with standard hardware. By having agent i take several snapshots of the wireless channel h_{ij} to another agent j as it moves over a piece-wise linear [7] or circular trajectory [8], a *signal profile* can be computed as:

$$F_{ij}(\phi, \theta) = \frac{1}{\left| \text{Eig}_n(\hat{h}_{ij} \hat{h}_{ij}^+) \exp \sqrt{-1} \Phi_{ij}(\phi, \theta) \right|^2}, \quad (5)$$

$$\{\phi_{\max}, \theta_{\max}\} = \arg \max_{\phi, \theta} F_{ij}(\phi, \theta) \quad (6)$$

An actual measured profile F_{ij} is shown in Fig. 2 for $\theta \in (-180, 180)$ and $\phi \in (0, 40)$, and the unit vector $v_{\theta_{\max}}(F_{ij})$ along the direction θ_{\max} is depicted in the schematic on the right hand side of Fig. 2. This captures the direction of arrival of the signal in 3D space between two communicating agents i and j where ϕ is the polar direction of the arriving signal (in the plane) and θ is the azimuthal direction of the arriving signal (out of the plane). Here the raw channel ratio between two antennas is used: $\hat{h}_{ij} = h_{1ij}/h_{2ij}$, a vector of the ratio of wireless channel snapshots between two antennas mounted on the body of the receiving robot j (Fig. 6 shows the two antennas used for communication and for measuring F_{ij}). The function $\Phi_{ij}(\phi, \theta)$ is defined as $\Phi_{ij}(\phi, \theta) = \frac{2\pi r}{\lambda} \cos(\phi - B_j) \sin(\theta - \Gamma_j)$, λ is the wavelength of the signal, r is the distance between the two antennas, B_j, Γ_j are the transmitters orientation, $\text{Eig}_n(\cdot)$ are noise eigenvectors, $(\cdot)^+$ is the conjugate transpose, and k is the number of signal eigenvectors, equal to the number of paths. In order for an agent i to obtain a profile F_{ij} , it is necessary to measure i 's displacement as it obtains several channel snapshots h_{ij} . In the current paper we use circular motion to obtain F_{ij} where the measuring robot i turns in place for a $1/4$ turn while obtaining wireless channel snapshots. Of particular importance to our approach is prior work which compares peak locations in the F_{ij} profile to derive a likelihood that a reported relative position between the agents i and j is correct [8]. Let $\mathcal{W}_{ij}(\phi_{ij}, \theta_{ij})$ be the likelihood that a transmitting agent i is indeed along its reported direction (ϕ_{ij}, θ_{ij}) with respect to a receiving agent j . The likelihood is derived as (cf. β in [8]):

$$\mathcal{W}_{ij}(\phi_{ij}, \theta_{ij}) = g(\phi_{ij} - \phi_{F_{ij}}; 0, \sigma_\phi^2) \times g(\theta_{ij} - \theta_{F_{ij}}; 0, \sigma_\theta^2) \quad (7)$$

where $\phi_{F_{ij}}$ and $\theta_{F_{ij}}$ denote the closest maximum in F_{ij} to $(\phi_{F_{ij}}, \theta_{F_{ij}})$ and $g(x; \mu, \sigma^2) = \min(1, \sqrt{2\pi} f(x; \mu, \sigma))$ is a normalized Gaussian PDF with mean μ and variance σ^2 . In this paper we will provide an experimental study of \mathcal{W}_{ij} , developing the necessary framework for integrating this likelihood into pose-graph optimization so that AOA can be used as an independent observation to detect outliers in relative position measurements between agents (Section 6).

5 Active Rendezvous

In this section we describe a framework for achieving active rendezvous between neighboring agents for keeping pose graph optimization errors below a desired threshold. As agents move through the environment, their pose estimation errors grow due to accumulated odometry and sensor error [9], but by exchanging

information and relative pose estimates, these errors can be reduced. We thus introduce: 1) a method for initiating a request for active rendezvous among agents as estimation errors grow beyond an acceptable threshold, 2) the subset of the underlying network of agents to be activated to complete an active rendezvous, and 3) the set of relative position commands, based on wireless signal profiles, to be executed by each robot in the subset to achieve communication rendezvous.

We assume each agent i is capable of monitoring its estimated pose error as shown in Algorithm 2, of which we introduce an example of in (4). This error function could be replaced with any generic error metric that measures the disagreement between pose estimates and measurements. Once this error passes a prescribed (arbitrary) threshold value of δ for any agent i , Algorithm 2 identifies a neighboring communication agent j which has the highest current signal-to-noise-ratio to agent i based on information sensed over the agents' shared wireless link ij and calls Algorithm 1. At this point, agent j will initiate active rendezvous with agent i starting at time t_l in order to satisfy the data rate q_i (in Mb/s) requested by agent i for data transfer. Integral to our development is a result found in [7] which derives an edge cost using AOA information over any link ij : $r_M(p_j, P_t, w_{ij}, F_{ij}) = (p'_{ij} - p_j)^T M_{ij} (p'_{ij} - p_j)$ which is a Mahalanobis distance between an agent j with position p_j and the "virtual" position, p'_{ij} , of agent i as determined from the AOA profile F_{ij} . In particular, minimizing this edge cost with respect to p_j returns a position for agent j that improves communication rate to i . Here, $p'_{ij} = p_j + w_{ij}v_{\theta_{\max}}$ is the perceived distance between agent i and j as estimated from the wireless profile F_{ij} and $v_{\theta_{\max}}$ is a vector along the maximum angle-of-arrival of the signal between i and j , and w_{ij} is the current service discrepancy of agent j to agent i . Here the matrix M_{ij} encodes the AOA information from the profile F_{ij} as $M_{ij} = Q_{ij}\Lambda Q_{ij}^T$ where $Q_{ij} = [v_{\theta_{\max}}, v_{\theta_{\max}^\perp}]$, $v_{\theta_{\max}}$ is a unit vector along the direction of maximum AOA (see Fig. 2 for a description of $v_{\theta_{\max}}$), and $\Lambda = \text{diag}(\frac{1}{\sigma^2}, 1)$ is a diagonal matrix capturing the noise characteristics of F_{ij} , and \perp denotes the orthogonal vector. The paper [7] shows how to derive the value of σ^2 from the profile F_{ij} however for simplicity here we will simply assume that $\sigma < 1$ which amounts to the link ij having more signal than noise. We define possible agent behaviors:

- *move_to_relative_waypoint*: Agent moves toward a given waypoint.
- *RandomWalk*: Agent moves along a randomly oriented trajectory.
- *AdaptiveWalk*: Agent takes a series of *move_to_relative_waypoint* using signal profiles.

All behaviors will result in new observation and poses estimates. Algorithm 1 describes how an active rendezvous is achieved for that agent when the pose estimation error reaches a critical threshold. Note that we do not assume line-of-sight to rendezvous in this case. During each iteration of this algorithm, the agent performing the rendezvous uses F_{ij} to obtain a new position $p_j(t+1)$ of agent j until a desired number of observations κ have been generated between itself and agent i for optimization.

After optimization, the agents revert back to *Random-Walk*-based exploration and update $\bar{z}_i(t)$ and pose estimates using sensor inputs (such as odometry, scan matching, etc). We describe an algorithm below that monitors the

Algorithm 1 ACTIVE RENDEZVOUS

Require: Desired data exchange rate q_i , pose error threshold δ , minimum number of observations κ , agent j selected for rendezvous, raw pose estimates x_i , some small positive values $\varepsilon > 0$

Ensure: Optimized pose estimates x_i^* , x_j^* , for agents i and j

```

1: while  $|z_i^j(t_l, t_k)| < \kappa$  do
2:    $w_{ij} \leftarrow \max\{0, \alpha_j \frac{q_i - \rho_{ij}}{q_i}\}$  ▷ compute service discrepancy
3:    $F_{ij} \leftarrow \text{Equation (5)}$ 
4:    $p'_{ij} \leftarrow p_j(t) + \gamma w_{ij} \mathbf{v}_{\theta_{\max}}(F_{ij})$  ▷ virtual client position
5:    $\nabla r_M = M_{ij}(p'_{ij} - p_j)$  ▷ Compute communication gradient direction
6:    $p_j(t+1) = p_j(t) + w_{ij} \nabla r_M$ 
7:    $[x_i, \bar{z}_i^j(t_l, t_k)] \leftarrow \text{move\_to\_relative\_waypoint}(p_j(t+1))$ 
8:    $\rho_{ij} \leftarrow \text{ESNR}_{ij}$  ▷ actual received signal strength in Mb/s over link  $ij$ 
9:   if  $q_i \leq \rho_{ij}$  then
10:     $q_i \leftarrow q_i + (\rho_{ij} - q_i) + \varepsilon$  ▷ Update data transfer rate to get enough  $\bar{z}_i^j$ 
11:   end if
12: end while
13:  $x_i^* \leftarrow \text{Equation (3)}$ 
14: return  $x_i^*$ 

```

error for each agent and controls the time at which the agent will trigger an active rendezvous request. Any agent executing the exploration task will continuously run the MONITOR algorithm below. The selection of adaptive agent j is based on signal-to-noise ratio (ESNR) of the shared link ij , and Algorithm 1 ACTIVE RENDEZVOUS will be triggered once the internal error Err_i exceeds the given threshold δ .

6 Outlier Rejection

The problem of detecting outlier measurements in graph-based localization is of major importance due to the detrimental effects outliers have on pose estimation. This section discusses how wireless communication channels can be used to reject outliers, i.e., relative pose measurements with large errors, in pose graph optimization. In particular, we devise a mathematical framework for using relative pose information captured in F_{ij} to scale the information matrix of each relative pose observation $\bar{z}_j^i(t)$ such that outlier measurements are much less likely to influence the maximum likelihood estimate.

We defined our observational model as (2) with the assumption that all observations were drawn from a Gaussian distribution. An *outlier* measurement however is not necessarily drawn from the same distribution as (2) and can introduce significant bias to an optimization [2]. Ideally it would be possible to automatically weigh outlier mea-

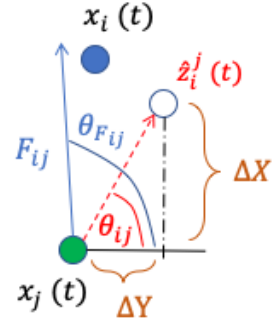


Fig. 3: Angle from F_{ij} versus angle from reported relative position θ_{ij} (2D).

Algorithm 2 ERROR MONITOR

Require: Estimated pose error threshold δ , agent index i , desired data exchange rate q_i , minimum number of observations κ , priority table for all agents α , minimum connected neighbors of i , \mathcal{N}_{C_i}

```

1:  $t \leftarrow 1, x_i \leftarrow \emptyset, \bar{z}_i \leftarrow \emptyset$  ▷ Initialization
2: while explore do
3:    $[x_i(t), \bar{z}_i(t)] \leftarrow \text{RandomWalk}$ 
4:    $\text{Err}_i(t, x_i(t), \bar{z}_i(t)) \leftarrow \text{Equation (4)}$ 
5:   if  $\text{Err}_i(t, x_i(t), \bar{z}_i(t)) > \delta$  then
6:      $\text{min\_service\_discrepancy} \leftarrow \infty$ 
7:     for  $j$  in  $\mathcal{N}_{C_i}$  do ▷ Selection of adaptive Agent j
8:        $\rho_{ij} \leftarrow \text{ESNR}_{ij}$ 
9:        $w_{ij} \leftarrow \alpha_i \frac{q_i - \rho_{ij}}{q_i}$ 
10:      if  $w_{ij} < \text{min\_service\_discrepancy}$  then
11:         $j^* \leftarrow j$ 
12:         $\text{min\_service\_discrepancy} \leftarrow w_{ij}$ 
13:      end if
14:    end for
15:     $x_i^* \leftarrow \text{Algorithm 1}(q_i, \delta, \kappa, j^*, x_i)$ 
16:  end if
17:   $x \leftarrow x_i^*$ 
18:   $t \leftarrow t + 1$ 
19: end while

```

surements less in the optimization of (4) by setting their information values to small or even zero values, thus mitigating their effect on the resulting pose estimation. The AOA information captured in an F_{ij} profile can be used for exactly this purpose. Formally, we want to verify that the observation $\bar{z}_j^i(t)$ is consistent with the observation model in (8). In addition to these observations, agents i and j have access to their signal profiles F_{ij} which also encode relative pose information through angle-of-arrival of the signal. We define (ϕ_{ij}, θ_{ij}) to be the relative position of agent i with respect to agent j which can be derived from the relative pose estimate \hat{z}_i^j (Fig. 3) as:

$$\theta_{ij} = \arctan 2(\Delta Y, \Delta X) \quad (8)$$

$$\phi_{ij} = \arctan 2(\Delta Z, \sqrt{\Delta X^2 + \Delta Y^2}) \quad (9)$$

The signal profile F_{ij} contains angle-of-arrival information for all incoming signal paths from i to j . A signal path along the direction (ϕ, θ) would result in a peak value of $F_{ij}(\phi, \theta)$. Therefore we can define the closest maximum peak location in F_{ij} to the reported relative position (ϕ_{ij}, θ_{ij}) as $(\phi_{F_{ij}}, \theta_{F_{ij}})$ where

$$[\phi_{F_{ij}}, \theta_{F_{ij}}] = \arg \min_{\phi, \theta} \alpha + \beta \quad (10)$$

$$s.t. \quad \|\theta - \theta_{ij}\| \leq \alpha, \|\phi - \phi_{ij}\| \leq \beta, (\phi, \theta) \in \Theta_N(F_{ij})$$

Here $\Theta_N(F_{ij})$ is the set of angles producing the N largest peaks in F_{ij} . In other words, $(\phi_{F_{ij}}, \theta_{F_{ij}})$ is the tuple of angles among the peaks of F_{ij} corresponding to the signal direction that is closest to the reported position (ϕ_{ij}, θ_{ij}) .

From Equation (7) in Section 4 we can compute the likelihood that agent ij is indeed at the reported relative location (ϕ_{ij}, θ_{ij}) according to the signal profile F_{ij} as $W_{ij} \in [0, 1]$. This likelihood serves as a natural candidate for a weighting term that can be applied to the information matrix Ω_{ij} of each relative measurement between agents. This would result in a smaller weight, nearing zero, for all relative pose measurements (ϕ_{ij}, θ_{ij}) that are likely to be outliers as reported by the AOA signal profile with computable variance $\sigma_\theta, \sigma_\phi$. However, given the high variance of the AOA signal in practice, we choose only to weight outliers over a certain threshold. For all relative pose observations, we compute a new information matrix $\Omega'_{\bar{z}_j^i}$ as:

$$\Omega'_{\bar{z}_j^i} := \begin{cases} W_{ij} \cdot \Omega_{\bar{z}_j^i} & |\theta_{ij} - \theta_{F_{ij}}| \geq \Delta \text{ or } |\phi_{ij} - \phi_{F_{ij}}| \geq \Delta \\ \Omega_{\bar{z}_j^i} & \text{otherwise} \end{cases} \quad (11)$$

where Δ is the error threshold past which we begin to weigh the observation, and W_{ij} is given by (7).

7 Results

In this section, we describe our both our simulation-based experiments as well as our experiments involving real robots. For each experiment we compare our proposed approach, *active rendezvous*, with a naive random rendezvous exploration strategy. For comparing accuracy we utilize the Absolute Trajectory Error (ATE) metric, a standard benchmark metric in the mapping community [23]. We use a specialized version of ATE that our chosen pose graph optimization implementation uses, which is defined as [4]:

$$ATE_{\text{trans}} := \frac{1}{\sum_{i=1}^n n_i} \sum_{i=1}^n \sum_{t=t_0}^{t_{n_i}} \|p_i(t) - \hat{p}_i(t)\|^2 \quad (12)$$

$$ATE_{\text{rot}} := \frac{1}{\sum_{i=1}^n n_i} \sum_{i=1}^n \sum_{t=t_0}^{t_{n_i}} \|R_i(t)^\top \hat{R}_i(t) - I_3\|_F^2 \quad (13)$$

where n_i is the number of poses in the trajectory of robot i , $p_i(t)$ and $R_i(t)$ are the estimated translation and rotation of robot i at time t , and $\hat{p}_i(t)$ and $\hat{R}_i(t)$ are benchmark positions and rotations of robot i , typically according to ground truth from motion capture.

7.1 Simulation Experiments

7.1.1 Setup: Our simulation implementation consisted of a framework developed based on the GTSAM library with ROS and *Gazebo* for agent control and visualization as shown in Fig. 4. Each agent’s virtual measurements and *Gazebo* pose data are fed to a custom backend optimizer based on a distributed mapping implementation by [4]. We were able to test our

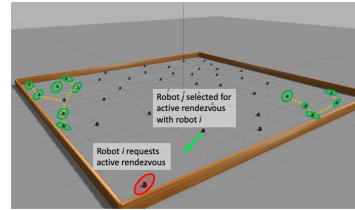


Fig. 4: *Simulation environment with 50 robots. Robots request active rendezvous when error grows beyond a desired threshold.*

framework through controlling virtual agents in the Gazebo simulations for performing active rendezvous. The assignment of the nearest active neighbor to a static agent was based on Euclidean distance so as to approximate the behavior of communication quality in real wireless profiles. A combined obstacle detection and avoidance system based on adaptive navigation emulation (using Gazebo environment’s noisy ground truth) and virtual LIDAR data was also tested before deploying it on actual robots.

7.1.2 Results: In order to examine the impact of our proposed *active rendezvous* approach, we first compared the estimation error of our approach with the naive random rendezvous based approach in the simulation environment described previously. These simulations allowed us to examine the result of our approach in larger groups of robots. We performed 10 trials, each with 50 agents, that ran for 50 iterations, with pose error threshold $\delta = 10$. We add Gaussian noise of 0.1 units in translation and 3° in rotation for generated poses and measurements. Each agent is capable of moving 2 units in one iteration and has a virtual sensor range of 2.2 units to generate measurements. The aggregate results in Fig. 5 show that while the random rendezvous approach performs similarly in estimation error to our proposed approach initially, our approach periodically enforces rendezvous over the experiment duration, providing better long-term performance.

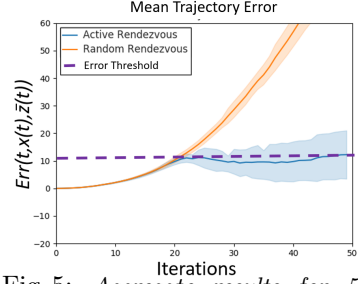


Fig. 5: Aggregate results for 50 agent simulation showing mean Error bounded at a desired threshold.

7.2 Hardware Experiments

7.2.1 Setup: For hardware experiments, two *Turtlebot3 Burger* robots (Figure 6) were used with MinnowBoard *Turbot* Dual and Quadcore off-the-shelf SBCs running Ubuntu 16.04 LTS with kernel v4.15 and two *5dBi* antennas spaced 22 cm apart, communicating over a 5 GHz channel. We attached an Intel 5300 Wi-Fi card to the Turbot which estimates wireless channels for each antenna via the 802.11n *Channel State Information*(CSI) tool [10]. A Matlab framework calculated wireless signal profiles (Sec. 4) and provided actuation commands to agents during adaptive navigation. An *Optitrack* motion capture system was used to collect ground truth pose data. The *Turbots* were set in monitor mode to broadcast fixed length ping packets at a rate of 200 packets/sec. Angle-of-arrival profiles were calculated based on CSI using ground truth orientation; this is also able to be done using an IMU sensor as shown by Gil et al in [7]. The measurements $\bar{z}_j^i(t)$ were generated by injecting noise from a zero-mean Gaussian distribution with standard deviation $\sigma_R = 5^\circ$

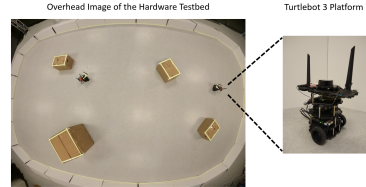


Fig. 6: Hardware Setup

for rotation and $\sigma_t = 0.2$ m for the translations to ground truth measurements as in Sec. 7.1.

7.2.2 Results: We compare our approach to random rendezvous with two sets of real-world experiments, designed both to validate our approach in hardware settings, and to demonstrate our active rendezvous approach works in the presence of obstacles. We first display the pose error $Err_i(t, x_i(t), \bar{z}_i(t))$ and rendezvous history for a single trial of hardware experiments in the environment with and without obstacles. It can be seen from Fig. 7 that early in the trial, the random rendezvous based approach performs similarly to our approach due to several random rendezvous. However, after a long period without a rendezvous, the random-walk based approach begins to diverge. In contrast, our method begins to enforce active rendezvous as soon as the pose error increases. Additionally, examining Fig. 7 (c),(d), we note that the presence of obstacles affects the number of rendezvous for the random-walk based approach while the number of rendezvous for our approach appears independent of obstacles.

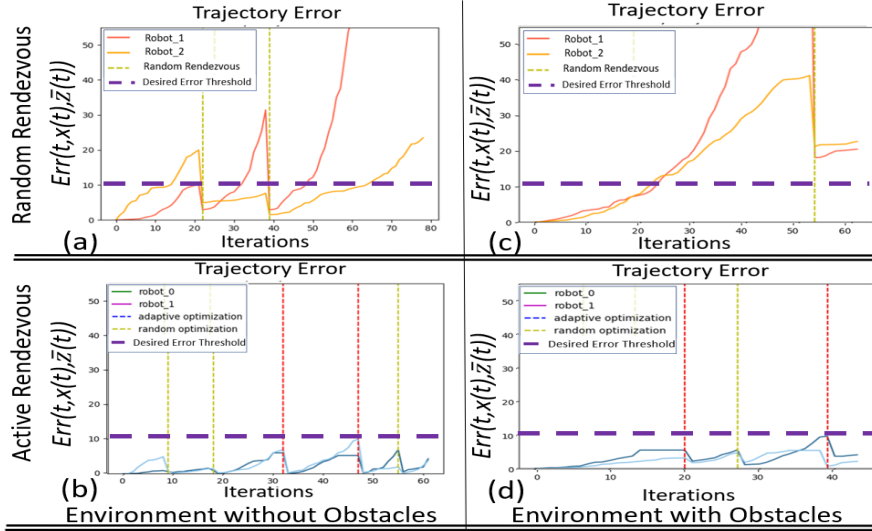


Fig. 7: Single trial of Random Rendezvous versus Active Rendezvous (Y-axis: Equation (4)). Active Rendezvous reduces error by 6X versus Random Rendezvous for different environments and platforms with heterogeneous sensor noise. Horizontal dashed lines indicate desired error threshold. Vertical lines indicate rendezvous opportunities.

The next set of experiments was performed in the environment shown in Fig. 6 without obstacles. We performed 6 trials that each ran for 50 iterations. We then introduced 4 obstacles and performed the same number of trials and iterations per trial in this environment. Aggregate results, as well as individual robot errors, for both experimental conditions are shown in Fig. 8. We see the same trends as in simulation: early on in the experiments, both methods show similar performance, but over time the random-walk based method degrades while our approach remains accurate. Finally, we performed identical hardware experiments, both with and without obstacles, in extreme low light conditions

(Fig. 9). These experiments were designed to showcase that our method of rendezvous is completely independent of visual conditions, in a dark, featureless environment which would severely inhibit vision-based place recognition algorithms for coordinating rendezvous

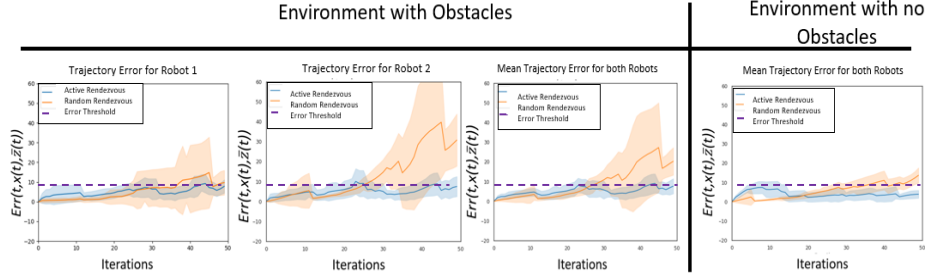


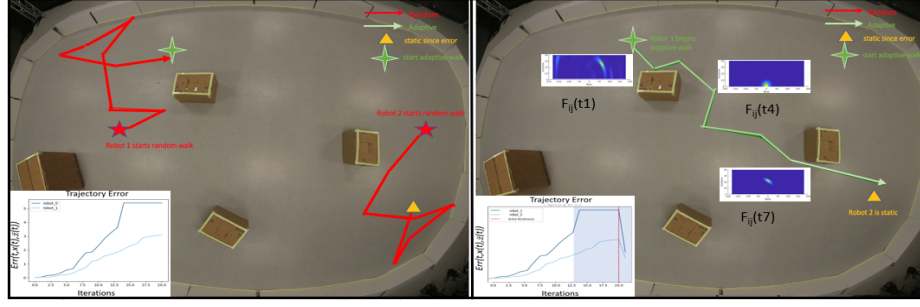
Fig. 8: Aggregate results for Random rendezvous vs. Active rendezvous over 10 trials of hardware experiments. Active rendezvous maintains error threshold for environments with and without obstacles.

7.3 Experimental Results for Outlier Rejection

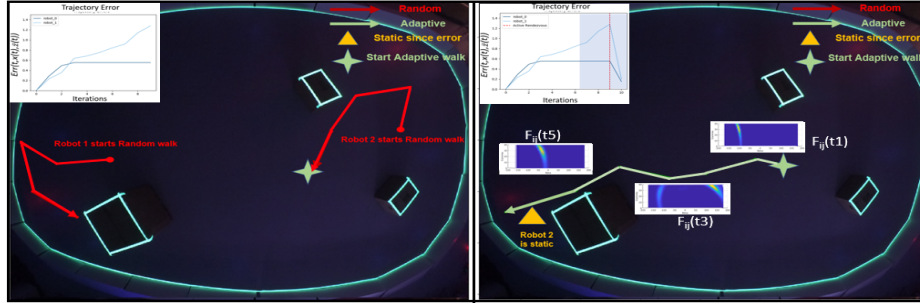
In this section we present hardware results for using CSI to detect and weight outlier measurements prior to performing optimization. The relative-pose measurements are generated by randomly injecting them with translation and rotation error between $(2\sigma \ 3\sigma)$ of the original noise distribution to obtain outliers. As explained in Sec. 6, we run 5 trials of active rendezvous and terminate each one after collecting 9 relative pose measurements between agents. The ground truth error in estimated trajectory before and after outlier rejection, along with the error distribution of 100 AOA measurements samples and plot of the joint-distribution of AOA and relative pose observations are shown in Figure 10. The average ground truth error is defined as the sum of Eqn. (12) and Eqn. (13). The \mathcal{W} in Fig. 10 (c) is computed from equation given in Sec. 6. The joint-distribution plot shows that the AOA measurements reliably detect outliers past 7.2° of difference, so we set our threshold $\delta \geq 7.2^\circ$ as the rejection boundary for outliers. From Fig. 10, it is clear that using AOA to reject observations leads to a significant decrease in average ground truth error. This reduction in error highlights the benefit of having an independent modality to confirm any relative pose measurements.

8 Conclusion

We have presented a method for integrating directional information from wireless communications into pose graph optimization that enables agents to rendezvous with one another independent of the environment and reject outlying relative pose observations. We demonstrate the utility of this method both in simulation and in hardware experiments. These experiments show that the use of *active rendezvous* results in an error reduction of 6X as compared to randomly occurring rendezvous and the use of CSI to reject outliers provides a reduction in error



(a) Error before and after rendezvous in well-lit conditions.



(b) Error before and after rendezvous in low-lighting conditions.

Fig. 9: Active rendezvous in a visually degraded environment where vision based rendezvous would fail. Testbed boundary is shown fluoresced (not visible to agents). Shaded regions of plots show adaptive navigation and Active rendezvous.

reduction of 32% as compared to no CSI information.

Acknowledgements: The authors gratefully acknowledge support by the NSF CAREER award number 1845225, MIT Lincoln Labs Line Grant, and the Fulton Undergraduate Research Initiative.

Disclaimer: DISTRIBUTION STATEMENT A. Approved for public release. Distribution is unlimited. This material is based upon work supported by the Under Secretary of Defense for Research and Engineering under Air Force Contract No. FA8702-15-D-0001. Any opinions, findings, conclusions or recommendations expressed in this material are those of the author(s) and do not necessarily reflect the views of the Under Secretary of Defense for Research and Engineering.

References

- [1] Cadena C, Carlone L, Carrillo H, Latif Y, Scaramuzza D, Neira J, Reid I, Leonard JJ (2016) Past, present, and future of simultaneous localization and mapping: Toward the robust-perception age. *Trans Rob* 32(6):1309–1332
- [2] Carlone L, Calafiore GC (2018) Convex relaxations for pose graph optimization with outliers. *IEEE Robotics and Automation Letters* 3(2):1160–1167
- [3] Carlone L, Du J, Ng MK, Bona B, Indri M (2014) Active slam and exploration with particle filters using kullback-leibler divergence. *Journal of Intelligent & Robotic Systems* 75(2):291–311

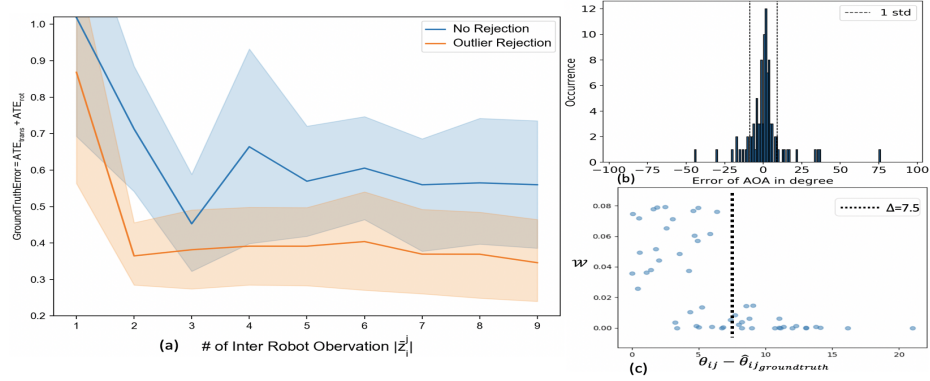


Fig. 10: The aggregate results over 5 Monte Carlo trials show 32% reduction in ground truth error by using AOA for outlier rejection.

- [4] Choudhary S, Carlone L, Nieto C, Rogers J, Christensen HI, Dellaert F (2017) Distributed mapping with privacy and communication constraints: Lightweight algorithms and object-based models. *The International Journal of Robotics Research* 36(12):1286–1311
- [5] Cunningham A, Wurm KM, Burgard W, Dellaert F (2012) Fully distributed scalable smoothing and mapping with robust multi-robot data association. In: *2012 IEEE International Conference on Robotics and Automation*, IEEE, pp 1093–1100
- [6] Fox D, Ko J, Konolige K, Limketkai B, Schulz D, Stewart B (2006) Distributed multirobot exploration and mapping. *Proceedings of the IEEE* 94(7):1325–1339
- [7] Gil S, Kumar S, Katabi D, Rus D (2015) Adaptive communication in multi-robot systems using directionality of signal strength. *The International Journal of Robotics Research* 34(7):946–968
- [8] Gil S, Kumar S, Mazumder M, Katabi D, Rus D (2017) Guaranteeing spoof-resilient multi-robot networks. *Auton Robots* 41(6):1383–1400
- [9] Grisetti G, Kuemmerle R, Stachniss C, Burgard W (2010) A tutorial on graph-based SLAM. *Intelligent Transportation Systems Magazine*, IEEE 2(4):31–43
- [10] Halperin D, Hu W, Sheth A, Wetherall D (2011) Tool release: Gathering 802.11n traces with channel state information. *ACM SIGCOMM CCR* 41(1):53
- [11] Howard A (2006) Multi-robot simultaneous localization and mapping using particle filters. *Int J Rob Res* 25(12):1243–1256
- [12] Khan UA, Kar S, Moura JM (2015) Linear theory for self-localization: Convexity, barycentric coordinates, and cayley–menger determinants. *IEEE Access* 3:1326–1339
- [13] Kretzschmar H, Stachniss C (2012) Information-theoretic compression of pose graphs for laser-based slam. *The International Journal of Robotics Research* 31(11):1219–1230

- [14] Kumar S, Gil S, Katabi D, Rus D (2014) Accurate indoor localization with zero start-up cost. In: Proceedings of the 20th Annual International Conference on Mobile Computing and Networking, ACM, New York, NY, USA, MobiCom '14, pp 483–494
- [15] Kumar S, Hamed E, Katabi D, Erran Li L (2014) Lte radio analytics made easy and accessible. In: Proceedings of the 2014 ACM Conference on SIGCOMM, ACM, New York, NY, USA, SIGCOMM '14, pp 211–222
- [16] Lazaro MT, Paz LM, Pinies P, Castellanos JA, Grisetti G (2013) Multi-robot slam using condensed measurements. In: 2013 IEEE/RSJ International Conference on Intelligent Robots and Systems, IEEE, pp 1069–1076
- [17] Lorincz K, Welsh M (2005) Motetrack: A robust, decentralized approach to rf-based location tracking. In: International Symposium on Location-and Context-Awareness, Springer, pp 63–82
- [18] Paull L, Huang G, Seto M, Leonard JJ (2015) Communication-constrained multi-auv cooperative slam. In: 2015 IEEE international conference on robotics and automation (ICRA), IEEE, pp 509–516
- [19] Piovani G, Shames I, Fidan B, Bullo F, Anderson BD (2013) On frame and orientation localization for relative sensing networks. *Automatica* 49(1):206–213
- [20] Roy N, Dudek G (2001) Collaborative robot exploration and rendezvous: Algorithms, performance bounds and observations. *Autonomous Robots* 11(2):117–136
- [21] Saeedi S, Trentini M, Seto M, Li H (2016) Multiple-robot simultaneous localization and mapping: A review. *Journal of Field Robotics* 33(1):3–46
- [22] Simmons RG, Apfelbaum D, Burgard W, Fox D, Moors M, Thrun S, Younes HLS (2000) Coordination for multi-robot exploration and mapping. In: Proceedings of the Seventeenth National Conference on Artificial Intelligence and Twelfth Conference on Innovative Applications of Artificial Intelligence, AAAI Press, pp 852–858
- [23] Sturm J, Engelhard N, Endres F, Burgard W, Cremers D (2012) A benchmark for the evaluation of rgb-d slam systems. In: 2012 IEEE/RSJ International Conference on Intelligent Robots and Systems, IEEE, pp 573–580
- [24] Todescato M, Carron A, Carli R, Schenato L (2015) Distributed localization from relative noisy measurements: A robust gradient based approach. In: 2015 European Control Conference (ECC), IEEE, pp 1914–1919
- [25] Valencia R, Miró JV, Dissanayake G, Andrade-Cetto J (2012) Active pose slam. In: 2012 IEEE/RSJ International Conference on Intelligent Robots and Systems, IEEE, pp 1885–1891
- [26] Vallvé J, Andrade-Cetto J (2015) Active pose slam with rrt. In: 2015 IEEE International Conference on Robotics and Automation (ICRA), IEEE, pp 2167–2173
- [27] Wang J, Katabi D (2013) Dude, where's my card?: Rfid positioning that works with multipath and non-line of sight. In: ACM SIGCOMM Computer Communication Review, ACM, vol 43, pp 51–62
- [28] Wei M, Aragues R, Sagues C, Calafiore GC (2014) Noisy range network localization based on distributed multidimensional scaling. *IEEE Sensors Journal* 15(3):1872–1883